



CHORUS

This is the accepted manuscript made available via CHORUS. The article has been published as:

Instability of bosonic topological edge states in the presence of interactions

Yaakov Lumer, Mikael C. Rechtsman, Yonatan Plotnik, and Mordechai Segev

Phys. Rev. A **94**, 021801 — Published 3 August 2016

DOI: [10.1103/PhysRevA.94.021801](https://doi.org/10.1103/PhysRevA.94.021801)

Instability of bosonic topological edge states in the presence of interactions

Yaakov Lumer¹, Mikael C. Rechtsman², Yonatan Plotnik¹, and Mordechai Segev¹

¹*Physics Department, Technion Israel Institute of Technology, Haifa 32000, Israel and*

²*Physics Department, The Pennsylvania State University, University Park, PA 16802, USA*

We analyze the stability of extended edge modes in a nonlinear (i.e. interacting) bosonic topological insulator. We see that these nonlinear modes are always unstable, despite the topological protection of edge modes in the linear system. For concreteness we use a photonic platform, but the results generalize to other bosonic systems. We give detailed description of the system in two extreme cases low nonlinearity and high nonlinearity, and discuss the breakup of the nonlinear edge states into solitons.

PACS numbers: 00.00.xx, 00.00.xx

Topological insulators represent a new class of materials, in which conduction of current is possible only on the surfaces/edges of the sample, but not inside it [1, 2]. In the two- and three-dimensional case, this conduction is robust and free of backscattering, arising from the so-called topological protection of the edge modes. In solid-state materials, such topological protection arises when significant spin-orbit coupling [3–5] or strong magnetic field are present [6], or in systems that are periodically modulated in time [7, 8]. The concept of topological protection is not restricted to electronic systems, and in the past few years there have been numerous works proposing to implement topological protection for other scenarios, such as photonic systems [9–12], acoustic waves [13] and optomechanical resonators [14]. Indeed, in the past few years topological phenomena have been observed in microwaves [15], photonics [16, 17], mechanical systems [18, 19], and ultracold atoms [20, 21]. Specifically in photonics, a topological insulator was implemented using an array of coupled helical waveguides [16], and independently by employing specific delay in a network of coupled optical cavities [17].

The discussion on the properties of topological insulators deals mainly with non-interacting systems. In Bose-Einstein condensates, this means that interactions between the particles are neglected, and in photonic systems this means that the optical power used to excite the system is relatively weak such that photon interaction is not mediated by the ambient medium (or alternatively, that the nonlinear response is sufficiently small). In bosonic systems (for example photonic systems) when local interactions are no longer negligible and there are a sufficient number of particles, the interactions can be modeled with a mean-field approach if they are strong enough, according to the Gross-Pitaevskii equation [22], also known as the cubic nonlinear Schrödinger equation [23, 24]. Indeed, there is a direct equivalence between the case of interacting Bose-Einstein condensates and nonlinear optical systems in that they are both described by the aforementioned equation. In fact, the Gross-Pitaevskii/Nonlinear Schrödinger equation arises as a limit of the Bose-Hubbard model and is completely universal: it should always be obeyed by interacting bosons in the mean-field limit. Thus, introducing nonlinearity

generalizes the treatment of topological systems to the interacting case potentially leading to fundamentally new phenomena. For example, nonlinearity was found to induce self-localized states that behave akin to topological edge modes of the small nonlinear defect they induce [25]. Also, in the regime of weak nonlinearity, it was shown that the nonlinearity can overcome the slight dispersion of the topological edge states, giving rise to long propagation distances without the spreading of the wavepacket [26]. Using quenching of a Zeeman field, it was shown that exponentially fast population of edge modes in ultracold boson systems can be achieved [27]. Nonlinear properties of topological edge states have also been studied in another Floquet topological insulator structure [28].

Here, we discuss the effects of nonlinearity on the stability of extended topological edge states, in the context of Floquet topological insulators. We show that such bosonic-type topological edge states are in fact unstable to interactions and will always break up - even the states with zero diffraction coefficient (inverse effective mass). We calculate the nonlinear dispersion of edge states with nonlinearity of various strengths, and show that, while for weak nonlinearities the spectrum coincides with that of the linear system, for stronger nonlinearity the spectrum of the edge states is starkly different. Depending on the strength of the nonlinearity, these edge states then break up to either bulk modes, or soliton-like wavepackets that can be either traveling or stationary. In contrast to the results of ref. [26], which apply to the regime of weak interactions, we always find the topological edge states to be unstable. These results do not contradict each other, since in the case of weak nonlinearity the solitons constitute the results of the breakup of the edge states. The specific physical context in which we present our results is the photonic system presented in [16]; however our results are universal - they can be easily generalized to other bosonic topological insulator systems in photonics [29, 30], cold-atom systems with mean-field interactions [31], exciton-polariton superfluids [32], and any system where bosonic physics is described by a nonlinear Schrödinger-type wave equation.

In our work we will focus on Floquet topological insulators, which have seen tremendous advancement in the past few years [7, 8, 33–35]. In Floquet topological

insulators, gauge fields are used in order to induce topological properties in otherwise non-topological systems by breaking time-reversal symmetry explicitly. Floquet topological insulators were first proposed in the context of condensed matter and electron transport [7, 8, 33, 34], where the gauge field was external electromagnetic radiation. The first realization of such Floquet topological insulator was implemented in photonics [16] in a system of coupled waveguides, arranged in a honeycomb lattice. The gauge field was introduced by rotating the waveguides in a helical fashion, causing an artificial gauge field to appear. A more recent realization of Floquet topological insulator was also implemented in cold-atom systems [20], where the gauge field was introduced by periodically moving the optical lattice.

We begin by describing our system under linear conditions. In the photonic topological insulator described in [16, 25], the system is a two-dimensional waveguide array arranged in a honeycomb lattice [36, 37]. We use the tight-binding model to describe our system, in which the wavefunction is described by the amplitudes at each waveguide. Our waveguides are arranged in a semi-infinite honeycomb lattice, terminated along one direction and infinite (or periodic) along the other direction. In this setting, eigenmodes of the system have a well-defined wavenumber along the periodic direction, which we will denote as the x -direction, while the direction in which the system is finite (i.e., is terminated by edges) will be denoted as the y -direction. An example of such a system, terminated in what is called a "zigzag edge" is shown in Fig. 1(a). To form a Floquet topological insulator, the waveguides have to spin around the propagation axis z at a given longitudinal frequency Ω and radius R (Fig. 1(a)). In the frame of reference in which the waveguides are stationary, the spinning of the waveguides can be described by introducing a vector potential $\mathbf{A}(z) = A_0 \cdot (\cos(\Omega z) \hat{x} + \sin(\Omega z) \hat{y})/a$ to the system [16, 25]. Here, a is the lattice constant, and $A_0 = k_0 \Omega R a$ is a measure of the spinning radius (k_0 is the wavenumber inside medium). Formally, our equation of motion is:

$$i\partial_z u_n(z) = \sum_{\langle m \rangle} c \cdot e^{i\mathbf{A}(z) \cdot \mathbf{r}_{mn}} u_m(z) \quad (1)$$

where the sum is over neighboring sites according to the honeycomb geometry, the coefficient c is the coupling constant between nearest neighbors, z is the propagation axis of the waveguides, and \mathbf{r}_{mn} is the displacement between waveguides m and n . For convenience, we set $c = 1$, without loss of generality.

In order to solve for the system's eigenvalues and eigenfunctions, we must first realize that there are no static eigenmodes, due to the fact that Eq. (1) is z -dependent. Instead, we can define Floquet eigenmodes of the system, based on the fact that in Eq. (1), written as $i\partial_z u_n(z) = \sum_{\langle m \rangle} H_{mn}(z) u_m(z)$, with the Hamiltonian $H_{mn}(z)$ is periodic with period $\Lambda = 2\pi/\Omega$ [7, 8]. The Floquet eigenmodes are $u_n(z) = e^{i\mu z} \varphi_n(z)$ with $\varphi_n(z)$ being Λ -periodic, and μ is the Floquet eigenvalue or 'quasi-

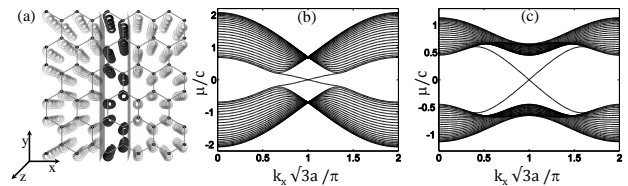


FIG. 1. (a) Honeycomb lattice, made from helical waveguides. The black waveguides between the two lines represent a unit cell in the x direction. (b) Spectrum of eigenmodes (in units of the coupling constant) for a finite lattice in the y direction, with $A_0 = 2$ and $\Omega = 10c$. (c) Same as (b), but with $A_0 = 3$ and $\Omega = 3c$.

energy'. In other words, Floquet modes obey Bloch-periodic boundary conditions in the temporal variable. Note that, by definition, the values of μ obey $-\Omega/2 \leq \mu < \Omega/2$. Thus, we can write $u_n(z + \Lambda) = u_n(z) e^{i\mu\Lambda}$, that is, the wavefunction $u_n(z)$ self-reproduces every Λ up to a phase. The spectrum of a semi-infinite system is calculated vs. k_x (the wavenumber in the periodic direction), where k_x is measured in the units of the inverse lattice constant in the x -direction, $\sqrt{3}a$. The spectrum using $\Omega = 10c$ and $A_0 = 2$ is shown in Fig. 1(b), and for a system with $\Omega = 3c$ and $A_0 = 3$ in Fig. 1(c). In both cases, we see two bands which populate the bulk modes, and between them mid-gap modes which are concentrated on the edges of the system, arising from the fact that the system is finite in the y -direction. These are the edge modes, and we see one mode for each edge top and bottom. Here, we will consider the two edges to be far apart such that there is no overlap between modes on different edges, which is valid assuming the lattice is sufficiently large. We emphasize three important properties, seen in the spectra of Fig. 1(b) and (c). First, is the fact that the edge modes have well-defined group velocity left or right, for the top and bottom edge, respectively. Second, the edge modes are deep in the bandgap, which means they are immune to scattering into the bulk for any type of elastic scattering. Finally, there is only one mode at a given energy on a given edge, meaning that these states must propagate robustly: there is no mode moving backwards into which backscattering can be possible. These three properties are the origin of the topological protection of edge modes, which means that propagating modes along the edge cannot be scattered or back reflected [1, 2, 30].

We now introduce interactions into the system, by adding a nonlinear term into the equation. The nonlinear term represents the mean-field interaction between bosonic cold-atom systems [22], as well as optical Kerr-type systems [23, 24]. Eq. (1) with the added term is now written as:

$$i\partial_z u_n(z) = \sum_{\langle m \rangle} H_{mn}(z) u_m(z) - \sigma |u_n(z)|^2 u_n(z) \quad (2)$$

where $\sigma = \pm 1$ denotes the sign of the nonlinearity (de-

terminated by whether atoms are attractive or repulsive, or whether the photonic nonlinear medium is of the focusing or defocusing type), and the strength of it is determined by the norm of the wavefunction, or the power, $P = \sum_n |u_n(z)|^2$, where the sum is over all sites in a unit cell, as shown in Fig. 1(a). We wish to solve for nonlinear eigenmodes of Eq. (2) in the Floquet sense - meaning solutions repeat themselves (up to a phase) after a period. Previous investigations of Eq. (2) in topological insulator systems found the existence of self-localized wave-packets (solitons) that rotate in accordance with topological nature of the underlying linear system [25], and approximate solutions for edge modes that use weak nonlinearity to overcome the dispersion in the edge-mode spectrum [26]. Also, an interacting topological insulator system made from ultracold bosons was considered in [27]. There, a nonlinear instability leads to exponentially fast population of edge modes when the system is initialized in a coherent state. However, instabilities of the edge modes themselves were outside the scope of the work. We look for nonlinear edge modes - extended solutions along x with a well-defined wavenumber k_x that are at the same time exponentially localized along the y direction. We find these solutions using the self-consistency method [25], in which the criteria for mode selection is the mode most localized on the edge.

In general, nonlinear waves are potentially subject to nonlinear instabilities. For extended waves, such instability is modulation instability (MI), in which small perturbations are amplified and reach the point where they break up the initial wave [38]. When the nonlinear wave breaks up, it can sometimes result in solitons, which are self-localized nonlinear solutions of Eq. (2). Generally, extended waves in a nonlinear self-focusing system tend to be unstable, if the dispersion is anomalous. In a periodic system (a lattice), extended states are subject to MI when the diffraction coefficient, (or inverse effective mass) ($D = m^{-1} = \partial^2 \mu / \partial k_x^2$) [23] and the nonlinearity have the same sign, e.g., when the nonlinearity is of the self-focusing type and the diffraction coefficient is positive. For a nonlinearity of the defocusing type, MI occurs for extended waves with negative diffraction coefficient [39–41]. It is important to note here that because the spectrum in our case is symmetric to $\mu \rightarrow -\mu$ (see Fig. 2(a) and (b)), for any region in the spectrum with positive D there exists an equivalent region with negative D . This property arises from the tight-binding approximation we use, and is only an approximate feature when more accurate models are considered. Because of this symmetry in the spectrum, any result we get with focusing nonlinearity ($\sigma = 1$) has a counterpart with the defocusing nonlinearity ($\sigma = -1$). This means that the sign of nonlinearity does not play a role in the results presented here, and for the rest of this article we choose to solve for $\sigma = 1$.

The new findings on topological systems raise a natural question: do the unique features associated with topological protection protect the topological edge states from

nonlinear instabilities? This question is further highlighted by the simple fact that the dispersion curve of mid-gap topological edge states exhibits regions of positive, negative and zero D . Specifically, the cases with negative D and zero D , which are cases where conventionally nonlinear instabilities are nonexistent [40, 41]. In the next paragraphs we show that any value of the nonlinearity gives rise to MI: the nonlinear edge modes of our system are always unstable and break up.

For concreteness, consider a helical waveguide array, with parameters $\Omega = 10$ and $A_0 = 2$ and for edges of the zigzag type. Here, we choose the work with the focusing nonlinearity $\sigma = 1$. It is important to emphasize that the results presented here are general, applicable to a wide range of parameters and to all three common types of edges in a honeycomb lattice (zigzag, bearded, arm-chair). We use low values of the nonlinearity ($P \leq 0.2$) in the results presented in Fig. 2, and we will describe results with strong nonlinearity in the next section. In Fig. 2(a) we show the nonlinear spectrum of the edge modes, together with the linear spectrum for ease of comparison, where each symbol corresponds to nonlinearity of different value. We see that the spectrum of the nonlinear edge modes is very similar to the spectrum of the linear edge modes, an unsurprising result that arises from the fact that the nonlinearity is weak. We then calculate the instability spectrum for each nonlinear mode. We do so by calculating the spectrum of weak modulations of the mode, and looking for modulations with an exponential blow-up. In Fig. 2(b) we plot the maximal exponential coefficient, f_{max} for the mode with $P = 0.05$. The results are essentially the same for all powers obeying $P \leq 0.2$.

For all values of nonlinearity discussed in this section, the modes are always unstable. This means that even for such low power levels, the topological modes are not protected against nonlinear instabilities. Physically, small modulations superimposed on the edge modes, through the nonlinearity, are coupled both to other edge modes and also to bulk modes. These modulations are then exponentially amplified until the original topological edge mode breaks up completely. For each mode, defined by its power and its wavenumber, the inverse of the values presented in Fig. 2(b) gives the typical propagation distance before the edge mode breaks up as a result of small, random fluctuations. Notably, even the mode at $k = \pi$, for which D is zero, exhibits nonlinear instability, as it can break into both bulk modes and other edge modes. This happens because the small modulations can couple to other bands, where modes with nonzero D exist at $k = \pi$. Had the band of edge modes been the only band in the spectrum, the specific topological edge mode with zero D would have been immune to the nonlinear instability [40, 41]. In Fig. 2(c) we plot the dynamics of such a break-up, for typical parameters of $k_x = \pi$ and $P = 0.05$. The pattern shown in this figure displays the intensity at the edge sites as a function of propagation distance. The lattice used in the calculations and presented in Fig. 2(c) has 40 unit cells, as represented in Fig 1(a), with periodic

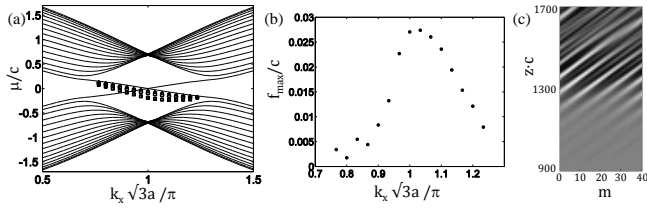


FIG. 2. Spectrum of nonlinear edge states, for low powers, with $A_0 = 2$ $\Omega = 10$. Plus signs: nonlinear edge modes for $P = 0.05$. Circles: nonlinear edge modes for $P=0.1$. Squares: nonlinear edge modes for $P=0.2$. Solid lines: underlying linear spectrum. (b) Instability spectrum for the nonlinear modes with $P = 0.05$. The y axis represents the exponential growth coefficient of noise, for each nonlinear edge mode. (c) Propagation simulation results for a nonlinear mode with $P = 0.05$. The figure presents intensity only on the edge. after a distance of $z = 1000$, the mode spontaneously breaks apart into solitons.

boundaries along x-axis. The horizontal axis in Fig 2(c) is the unit-cell index, and the vertical axis is the propagation distance, normalized using the coupling distance. In Fig. 2(c) we see that even for such low powers, the modes break up into soliton-like modes, which propagate on the edge, as predicted in [26]. These solitons exist only for weak nonlinearities, in which the nonlinearity compensates for dispersion arising from the small curvature in the dispersion curve in Fig. 2(a).

In Fig. 3, we present results calculated with strong values of nonlinearity, corresponding to $P \geq 0.5$, with $\Omega = 10$ and $A_0 = 2$. The spectrum of the nonlinear modes is presented in Fig 3(a), where each symbol represents modes with different value of nonlinearity. We see that in these cases, the spectrum of the nonlinear edge modes no longer resembles that of the spectrum of the linear modes, but takes completely different shape. In particular, we see that the range in momentum space in which edge modes exists differs from the linear case, and there are cases where nonlinear edge modes cover the whole Brillouin zone (for example, $P = 3$) unlike in the linear case, where they cover only $\frac{1}{3}$ of the momentum space. We also note that for each k_x value, the spectrum of the nonlinear edge modes never coincides with the spectrum of linear bulk modes. We calculate the instability spectrum in a similar fashion as the case with weak nonlinearities, which is presented in Fig. 3(b). Even here, we see that all the modes are unstable that even with a very small perturbation, they are bound to break up. The pattern shown in 3(c) shows the outcome of such a break-up, for typical parameters of $k_x = \pi$, propagation distance of $z = 150$, and $P = 3$. As shown in this figure, after a certain distance, every extended edge mode breaks up into several isolated, single site modes. These are in fact single-site solitons, in which the nonlinearity is so strong that they do not couple to neighboring sites at all. We understand these results by noting that for such high nonlinearities, the potential at each site changes significantly, to the point where the lin-

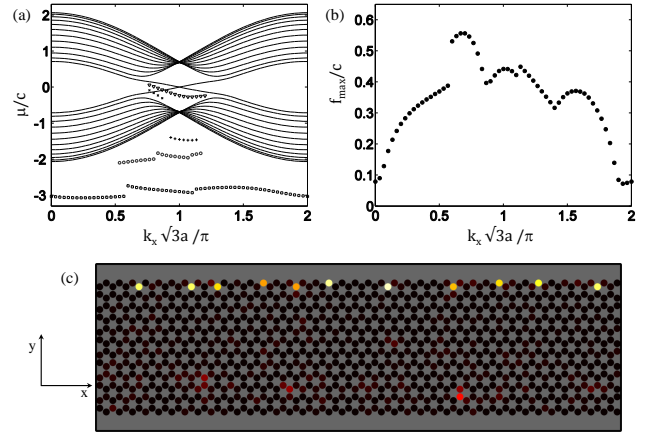


FIG. 3. Spectrum of nonlinear edge states, for high powers, with $A_0 = 2$ $\Omega = 10$. Triangles: nonlinear edge modes for $P = 0.25$. x signs: nonlinear edge modes for $P = 0.75$. Plus signs: nonlinear edge modes for $P = 1.5$. Circles: nonlinear edge modes for $P = 2$. Squares: nonlinear edge modes for $P = 3$. solid lines: underlying linear spectrum. (b) Instability spectrum for the nonlinear modes with $P = 3$. The y axis represents the exponential growth coefficient of noise, for each nonlinear edge mode. (c) Propagation simulation results for a nonlinear mode with $P = 3$. The figure presents the intensity pattern of the whole lattice after propagating a distance of $z = 150$. The existence of solitons, residing on single site is evident.

ear bulk band structure is very non-resonant. We confirm this observation by noting that the propagation constant of such soliton-like wavepackets does not lie in the topological band gap. If it were, we would expect behavior closely connected with topological edge-modes, such as unidirectional energy flow [25]. Instead, the propagation constant lies in the semi-infinite gap above the upper band, which is wrapped around to the bottom of the lower band due to the periodicity of the system.

Before closing, we consider the effects of losses on the results presented here. Losses are natural to almost any system (including photonic systems and cold-atom systems). Due to the nonlinear nature of the instability discussed here, losses which cause the wave to dissipate power will naturally cause any nonlinear effect to diminish. Specifically, if the loss coefficient in the system is greater than the exponential factor of the modulations, the wave will dissipate power too fast for the modulations to significantly affect it, rendering it stable. If, on the other hand, the losses are small, then nonlinear dynamics will qualitatively behave as though there is no loss - that is, the nonlinear wave will experience modulation instability. Here it should be emphasized in both photonic and cold-atom systems, losses can be managed to a high degree, making the observation of nonlinear phenomena ubiquitous.

In conclusion, we have studied the nonlinear properties

of edge modes in a model of a photonic Floquet topological insulator; we have analyzed their stability properties in two regimes - weak nonlinearity and strong nonlinearity, and have shown that in both regimes the modes are always unstable. Specifically, we have shown that the topological nature of the linear spectrum does not give rise to stable edge states. We have shown that the modes, under certain circumstances, break up into soliton-like wavepackets. When the nonlinearity is weak, wavepackets break up into solitons in which the weak nonlinearity compensates for the small dispersion of the edge mode spectrum. When the nonlinearity is strong, wavepackets break up into solitons that are guided in a single

waveguide, where the coupling to the linear bulk modes is very non-resonant. While our results are presented in the language of optical waveguide systems, they are applicable to other bosonic systems in which interactions can be modeled via a nonlinear Gross-Pitaevskii-type term, such as Bose-Einstein condensate systems and exciton-polariton condensates.

This research was supported by the Transformative Science Program of the Binational USA/Israel Science Foundation (BSF) and by the Israeli ICore Excellence Center Circle of Light. M.C.R. acknowledges the support of the National Science Foundation under grant number ECCS-1509546.

-
- [1] M. Z. Hasan and C. L. Kane, “Colloquium: Topological insulators,” *Reviews of Modern Physics* **82**, 3045–3067 (2010).
- [2] B. A. Bernevig and T. L. Hughes, *Topological Insulators and Topological Superconductors* (Princeton University Press, 2013).
- [3] C. L. Kane and E. J. Mele, “Quantum Spin Hall Effect in Graphene,” *Physical Review Letters* **95**, 226801 (2005).
- [4] B. A. Bernevig, T. L. Hughes, and S.-C. Zhang, “Quantum Spin Hall Effect and Topological Phase Transition in HgTe Quantum Wells,” *Science* **314**, 1757–1761 (2006).
- [5] M. König, S. Wiedmann, C. Brune, A. Roth, H. Buhmann, L. W. Molenkamp, X.-L. Qi, and S.-C. Zhang, “Quantum Spin Hall Insulator State in HgTe Quantum Wells,” *Science* **318**, 766–770 (2007).
- [6] K. v Klitzing, G. Dorda, and M. Pepper, “New method for high-accuracy determination of the fine-structure constant based on quantized Hall resistance,” *Physical Review Letters* **45**, 494–497 (1980).
- [7] T. Kitagawa, E. Berg, M. Rudner, and E. Demler, “Topological characterization of periodically driven quantum systems,” *Physical Review B* **82**, 235114 (2010).
- [8] N. H. Lindner, G. Refael, and V. Galitski, “Floquet topological insulator in semiconductor quantum wells,” *Nature Physics* **7**, 490–495 (2011).
- [9] Z. Wang, Y. Chong, John Joannopoulos, and Marin Soljacic, “Reflection-Free One-Way Edge Modes in a Gyromagnetic Photonic Crystal,” *Physical Review Letters* **100**, 013905 (2008).
- [10] R. O. Umucalilar and I. Carusotto, “Artificial gauge field for photons in coupled cavity arrays,” *Physical Review A* **84**, 043804 (2011).
- [11] M Hafezi, E. A. Demler, M. D. Lukin, and J. M. Taylor, “Robust optical delay lines with topological protection,” *Nature Physics* **7**, 907–912 (2011).
- [12] A. B. Khanikaev, S. Hossein Mousavi, W.-K. Tse, M. Kargarian, A. H. MacDonald, and G. Shvets, “Photonic topological insulators,” *Nature Materials* **12**, 233–239 (2012).
- [13] Zh. Yang, F. Gao, X. Shi, X. Lin, Z. Gao, Y. Chong, and B. Zhang, “Topological acoustics,” *Physical Review Letters* **114**, 114301 (2015).
- [14] M. Schmidt, S. Kessler, V. Peano, O. Painter, and F. Marquardt, “Optomechanical creation of magnetic fields for photons on a lattice,” *Optica* **2**, 635 (2015).
- [15] Z. Wang, Y. Chong, J. D. Joannopoulos, and M. Soljacic, “Observation of unidirectional backscattering-immune topological electromagnetic states,” *Nature* **461**, 772–775 (2009).
- [16] M. C. Rechtsman, J. M. Zeuner, Y. Plotnik, Y. Lumer, Da. Podolsky, F. Dreisow, S. Nolte, M. Segev, and A. Szameit, “Photonic Floquet topological insulators,” *Nature* **496**, 196–200 (2013).
- [17] M. Hafezi, S. Mittal, J. Fan, A. Migdall, and J. M. Taylor, “Imaging topological edge states in silicon photonics,” *Nature Photonics* **7**, 1001–1005 (2013).
- [18] R. Ssstrunk and S. D. Huber, “Observation of phononic helical edge states in a mechanical topological insulator,” *Science* **349**, 47–50 (2015).
- [19] L. M. Nash, D. Kleckner, A. Read, V. Vitelli, A. M. Turner, and W. T. M. Irvine, “Topological mechanics of gyroscopic metamaterials,” *Proceedings of the National Academy of Sciences* **112**, 14495–14500 (2015).
- [20] G. Jotzu, M. Messer, R. Desbuquois, M. Lebrat, T. Uehlinger, D. Greif, and T. Esslinger, “Experimental realization of the topological Haldane model with ultracold fermions,” *Nature* **515**, 237–240 (2014).
- [21] M. Aidelsburger, M. Lohse, C. Schweizer, M. Atala, J.T. Barreiro, S. Nascimbne, N.R. Cooper, I. Bloch, and N. Goldman, “Measuring the Chern number of Hofstadter bands with ultracold bosonic atoms,” *Nature Physics* **11**, 162–166 (2014).
- [22] Y. Castin, “Bose-Einstein condensates in atomic gases: simple theoretical results,” arXiv preprint arXiv:cond-mat/0105058 (2001).
- [23] F. Lederer, G. I. Stegeman, D. N. Christodoulides, G. Asanto, M. Segev, and Y. Silberberg, “Discrete solitons in optics,” *Physics Reports* **463**, 1–126 (2008).
- [24] S. Longhi, “Quantum-optical analogies using photonic structures,” *Laser & Photonics Review* **3**, 243–261 (2009).
- [25] Y. Lumer, Y. Plotnik, M. Rechtsman, and M. Segev, “Self-Localized States in Photonic Topological Insulators,” *Physical Review Letters* **111**, 243905 (2013).
- [26] M. J. Ablowitz, C. W. Curtis, and Y.-P. Ma, “Linear and nonlinear traveling edge waves in optical honeycomb lattices,” *Physical Review A* **90** (2014), 10.1103/PhysRevA.90.023813
- [27] B. Galilo, H. K. K. Lee, and R. Barnett “Selective pop-

- ulation of edge states in a 2D topological band system,” *Physical Review Letters* **115**, 245302 (2015)
- [28] Daniel Leykam and Y. D. Chong, “Edge Solitons in Non-linear Photonic Topological Insulators,” arXiv preprint arXiv:1605.09501 (2016).
- [29] K. Fang, Z. Yu, and S. Fan, “Realizing effective magnetic field for photons by controlling the phase of dynamic modulation,” *Nature Photonics* **6**, 782–787 (2012).
- [30] L. Lu, J. D. Joannopoulos, and M. Soljacic, “Topological photonics,” *Nature Photonics* **8**, 821–829 (2014).
- [31] I. Bloch and W. Zwerger, “Many-body physics with ultracold gases,” *Reviews of Modern Physics* **80**, 885–964 (2008).
- [32] A. Amo, S. Pigeon, D. Sanvitto, V. G. Sala, R. Hivet, I. Carusotto, F. Pisanello, G. Lemenager, R. Houdre, E. Giacobino, C. Ciuti, and A. Bramati, “Polariton Superfluids Reveal Quantum Hydrodynamic Solitons,” *Science* **332**, 1167–1170 (2011).
- [33] T. Oka and H. Aoki, “Photovoltaic Hall effect in graphene,” *Physical Review B* **79**, 081406(R) (2009).
- [34] Z. Gu, H. A. Fertig, D. P. Arovas, and A. Auerbach, “Floquet Spectrum and Transport through an Irradiated Graphene Ribbon,” *Physical Review Letters* **107**, 216001 (2011).
- [35] Y. H. Wang, H. Steinberg, P. Jarillo-Herrero, and N. Gedik, “Observation of Floquet-Bloch States on the Surface of a Topological Insulator,” *Science* **342**, 453–457 (2013).
- [36] O. Peleg, G. Bartal, B. Freedman, O. Manela, M. Segev, and D. Christodoulides, “Conical Diffraction and Gap Solitons in Honeycomb Photonic Lattices,” *Physical Review Letters* **98**, 103901 (2007).
- [37] Y. Plotnik, M. C. Rechtsman, D. Song, M. Heinrich, J. M. Zeuner, S. Nolte, Y. Lumer, N. Malkova, J. Xu, A. Szameit, Zh. Chen, and M. Segev, “Observation of unconventional edge states in photonic graphene,” *Nature Materials* **13**, 57–62 (2013).
- [38] V.E. Zakharov and L.A. Ostrovsky, “Modulation instability: The beginning,” *Physica D: Nonlinear Phenomena* **238**, 540–548 (2009).
- [39] D. N. Christodoulides and R. I. Joseph, “Discrete self-focusing in nonlinear arrays of coupled waveguides,” *Optics letters* **13**, 794–796 (1988).
- [40] Y. S. Kivshar and M. Peyrard, “Modulational instabilities in discrete lattices,” *Physical Review A* , 3198 (1992).
- [41] B. Wu and Q. Niu, “Superfluidity of BoseEinstein condensate in an optical lattice: LandauZener tunnelling and dynamical instability,” *New Journal of Physics* **5**, 104 (2003)